

COLLECTIVE NETWORK OF EVOLUTIONARY BINARY CLASSIFIERS FOR POLARIMETRIC SAR IMAGES

Serkan Kiranyaz⁽¹⁾, Stefan Uhlmann⁽¹⁾, Turker Ince⁽²⁾ and Moncef Gabbouj⁽¹⁾,

⁽¹⁾ Tampere University of Technology, P.O. Box 553 33101 Tampere FINLAND, Email: {firstname.lastname}@tut.fi

⁽²⁾ Izmir University of Economics, 35330 Balçova-Izmir TURKEY, Email: {firstname.lastname}@ieu.edu.tr

ABSTRACT

In this paper, we propose a collective network of (evolutionary) binary classifiers (CNBC) to achieve feature/class scalability, feature selection and classifier evolution for efficient classification of polarimetric SAR images. The main goal is to maximize the classification performance even though the training (ground truth) data may not be entirely accurate. The CNBC basically adopts a “Divide and Conquer” type approach by allocating several network of binary classifiers (NBCs) to discriminate each class and performing evolutionary search to find the optimal binary classifier (BC) in each NBC. Both visual and numerical performance evaluations of the proposed CNBC on the well-known AIRSAR San Francisco Bay and Flevoland, NL datasets demonstrate its superiority and a significant performance gap against other classifiers in this field.

1. INTRODUCTION

The accurate classification of the polarimetric synthetic aperture radar (SAR) images is a major and challenging task. This has been an active research area for the last three decades and the efforts can mainly be divided into three groups. The first type is the classification based on physical scattering mechanisms inherent in data such as the pioneer works of [18] and [26]. The second type is based on statistical characteristics of data, e.g. [14] and [20], and the most recent attempts belong to the image processing techniques such as [19] and [21]. There are also some hybrid approaches such as [14] and [18], which combine some of the aforementioned types. In general they can further be divided into supervised or unsupervised methods, their performance and suitability usually depend on applications and the availability of ground truth data. The supervised methods usually achieve higher classification accuracy compared to the unsupervised ones, however, providing a reliable ground-truth data might be cumbersome.

Main focus has been drawn on the supervised techniques using classifiers with non-linear operators such as artificial neural networks (ANNs) and hence it is not surprising that ANN based methods recently proposed, e.g. [2], [6], [23] and [24], for classification of SAR or high resolution remote sensing data have been shown to outperform other clustering techniques. Yet designing an optimal ANN for the problem in hand is a

crucial and challenging task. For instance, an ANN with no or too few hidden nodes may not differentiate among complex patterns, instead leading to only a linear estimation of such –possibly non-linear – problem. In contrast, if the ANN has too many nodes/layers, it might be affected severely by the noise in data due to over-parameterization, which eventually leads to a poor generalization or training. On such complex networks proper training may be infeasible and/or highly time-consuming. The optimum number of hidden nodes/layers might depend on input/output vector sizes, training and test data sizes, more importantly the characteristics of the problem, e.g. its non-linearity, dynamic nature, etc. In those works where a single (fixed) classifier is used, the overall performance directly depends on the choice of the classifier and its parameters. Furthermore, the feature set and the number of classes are usually kept as limited as possible not to cause the aforementioned feasibility problems on training process due to the increased complexity and well-known “curse of dimensionality” phenomenon. For this purpose, it is common to select only certain subset of features whilst discarding the others or to apply feature dimension reduction techniques such as principal component analysis (PCA). It is also worth mentioning that such systems are also static, that is, any update on either input or output layer (e.g. insertion of a new class or feature) will make the classifier useless and require setting up a new classifier from scratch.

In order to address these problems and hence to maximize the classification accuracy, in this paper we propose a global network structure, which is designed to seek for optimal classifier architecture for each distinct class type and feature set whilst utilizing a large set of major features within. Specifically in this approach, the following objectives will be targeted:

- I. *Evolutionary Search*: seeking for the optimum network architecture among a collection of configurations (the so-called Architecture Space, AS).
- II. *Evolutionary Update in the AS*: keeping only “the best” individual configuration in the AS among indefinite number of evolution runs.
- III. *Feature Scalability*: support for varying number of features. Any feature can be dynamically integrated without requiring a full-scale set-up and re-evolution.

- IV. *Class Scalability*: support for varying number of classes. Any class can dynamically be inserted without requiring a full-scale set-up and re-evolution.
- V. *High efficiency* for the evolution (or training) process: using as compact and simple classifiers as possible in the AS.
- VI. *Online (incremental) Evolution*: continuous online/incremental training (or evolution) sessions can be performed to improve the classification accuracy.
- VII. *Parallel processing*: classifiers can be evolved using several processors working in parallel.

In order to achieve all these objectives, we adopt a *Divide and Conquer* type of approach, which is based on a novel structure encapsulating a *network of (evolutionary) binary classifiers* (NBCs). Each NBC is devoted to a unique class and further encapsulates a set of *evolutionary Binary Classifiers* (BCs), each of which is optimally chosen within the AS, discriminating the class of the NBC with a unique feature set (or sub-feature). The optimality *therein* can be set with a user-defined criterion. The proposed *Collective NBC* (CNBC) structure currently supports two common ANN types as the underlying evolutionary binary classifiers, the Multi-Layer Perceptrons (MLPs) and the Radial Basis Function (RBF) networks because they are well-known and widely used in many applications. The recently proposed multi-dimensional Particle Swarm Optimization (MD-PSO) [9], [10] is used as the evolution technique for the MLP or RBF BCs whereas the exhaustive search with numerous runs of the Back-Propagation method may be applied as an alternative. The CNBC framework is developed over a dedicated application with a proper user-interface (UI) where the user can define new classes, or update the existing ones, whilst specifying the ground truth data (GTD) over a SAR image. Once the evolution process is completed for all individual BCs in all NBCs, CNBC can then be used to classify the entire SAR image with the predefined classes.

The rest of the paper is organized as follows. Section 2 presents the proposed CNBC structure along with the evolutionary update mechanism. Section 3 makes a brief introduction to the basic theory of polarimetric SAR and presents the major features used. Section 4 provides classification results over the fully polarimetric SAR images San Francisco Bay and Flevoland and performs comparative evaluations with major classifiers. Finally, Section 5 concludes the paper and discusses topics for future work.

2. COLLECTIVE NETWORK OF EVOLUTIONARY BINARY CLASSIFIERS

To achieve the third and fourth objectives mentioned earlier, i.e. the scalability with respect to a varying number of classes and features, a novel structure encapsulating a *network of binary classifiers* (NBCs) is developed, where

NBCs can *evolve* continuously with the ongoing evolution sessions i.e. using the user supplied ground truth data (GTD). Each NBC corresponds to a *unique* SAR terrain class and shall contain varying number of *evolutionary binary classifiers* (BCs), such as the widely known MLPs or RBFs, in the input layer where each BC performs binary classification using a single (sub-) feature. Therefore, whenever a new feature is extracted, its corresponding BC will be created, evolved (using the available GTD logs so far), and inserted into each NBC, yet keeping each of the other BCs “as is”. On the other hand, whenever an existing feature is removed, the corresponding BC is simply removed from each NBC in the system. In this way *scalability* with respect to any number of features is achieved and the overall system can avoid re-evolving from scratch.

Each NBC has a “fuser” BC in the output layer, which collects and fuses the binary outputs of all BCs in the input layer and generates a single binary output, indicating the relevancy of each FV to the NBC’s corresponding class. Furthermore, CNBC is also *scalable* to any number of classes since whenever a new class is defined by the user, a new NBC can simply be created (and evolved) only for this class without requiring any need for change or update on the other NBCs. This way the overall system dynamically adapts to user demands for varying number of SAR classes. As shown in *Figure 1*, the main idea in this approach is to use as large number of classifiers as necessary, so as to divide a massive learning problem into many NBC units along with the BCs within, and thus prevent the need of using complex classifiers as the performance of both training and evolution processes degrades significantly as the complexity rises due to the *curse of dimensionality*. A major benefit of our approach with respect to efficient training and evolution process is that the configurations in the AS can be kept as *compact* as possible avoiding unfeasibly large storage and training time requirements. This is a significant advantage especially for the training methods performing local search, such as BP since the amount of deceiving local minima is significantly lower in the error space for such simple and compact ANNs. Furthermore, when BP is applied exhaustively, the probability of finding the optimum solution is significantly increased. Also note that evolving the CNBC may reduce the computation time significantly since it contains simple and compact classifier networks, each of which can be individually evolved by a separate CPU (recall the objective VII– Parallel Processing) and hence the overall computation time can be reduced as much as desired on class level, which in practice will significantly lower computation time compared to training a single, static but complex ANN classifier.

The evolution of a subset of the NBCs or the entire CNBC is performed for each NBC individually with a two-phase operation, as illustrated in *Figure 2*. As explained earlier, using the feature vectors (FVs) and the target class vectors (CVs) of the training dataset, the evolution process of each BC in a NBC is performed within the current architecture

space (AS) in order to find the best (optimal) BC configuration with respect to a given criterion (e.g. training/validation MSE or classification error, CE). During the evolution, only NBCs associated with those classes represented in the training dataset are evolved. If the training dataset contains new classes, which do not yet have a corresponding NBC, a new NBC is created for each, and evolved using the training dataset.

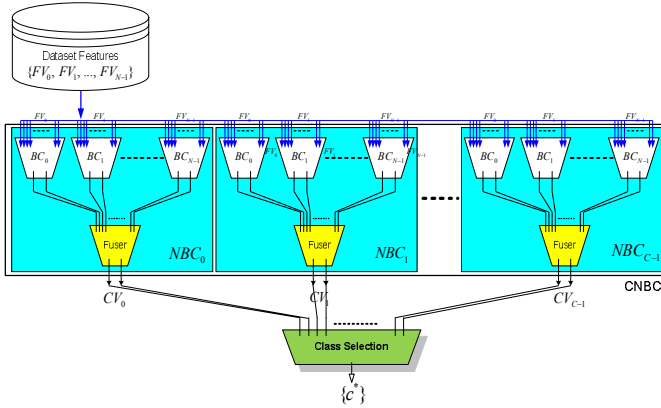


Figure 1: Topology of the proposed CNBC framework with C classes and N FVs.

In Phase 1, see top of Figure 2, the BCs of each NBC are first evolved given an input set of FVs and a target CV. Recall that each CV is associated with a unique NBC and the fuser BCs are not used in this phase. Once an evolution session is over, the AS of each BC is then recorded so as to be used for potential (incremental) evolution sessions in the future.

Recall that each evolution process may contain several runs and according to the aforementioned evolutionary update rule, the best configuration achieved will be used as the classifier. Hence once the evolution process is completed for all BCs in the input layer (Phase 1), the best BC configurations are used to forward propagate all FVs of the items in the training dataset to compose the FV for the fuser BC from their output CVs, so as to evolve the fuser BC in the second phase. Apart from the difference in the generation of the FVs, the evolutionary method (and update) of the fuser BC is same as any other BC has in the input layer. In this phase, the fuser BC *learns* the *significance* of each individual BC (and its feature) for the discrimination of that particular class. This can be viewed as the adaptation of the entire feature space to discriminate a specific class in a large dataset, or in other words, a crucial way of applying an efficient *feature selection* scheme as some FVs may be quite discriminative for some classes whereas others may not and the fuser, if properly evolved and trained, can “weight” each BC (with its FV), accordingly. In this way the usage of each feature (and its BC) shall optimally be “fused” according to their discrimination power of each class. Similarly, each BC in the first layer shall in time learn the significance of individual feature components of the corresponding FV for the discrimination of its class. In short the CNBC, if properly evolved, shall learn the significance (or the

discrimination power) of each FV and its individual components.

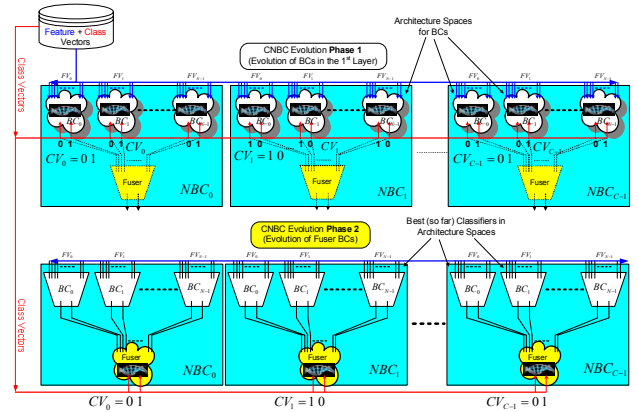


Figure 2: Illustration of the two-phase evolution session over BCs' architecture spaces in each NBC.

3. POLARIMETRIC SAR DATA PROCESSING

Polarimetric SAR (PolSAR) features can generally be divided into two categories: the first group belongs to the features extracted directly from the polarimetric SAR data and its different transforms such as the scattering matrix, and from which the Kennaugh matrix, the polarimetric coherency and covariance matrices, can be derived; whereas the second group is based on the polarimetric target decomposition theorems, which are used to extract information about scattering mechanisms in PolSAR. The coherent decomposition theorems such as the Pauli decomposition [4], the Krogager decomposition [11], the Cameron decomposition [3], and SDH (Sphere, Diplane, Helix) decomposition [12] aim to express the measured scattering matrix by the radar as the combination of scattering responses of coherent scatterers. In the other category, the incoherent decomposition theorems such as the Freeman decomposition [7], the Huynen decomposition [8], and the Cloude-Pottier (eigenvector-eigenvalue or $H/\alpha/A$) decomposition [4] employ the second order polarimetric representations of PolSAR data (such as covariance or coherency matrices) to characterize distributed scatterers. Each feature has its own strength and weaknesses for discriminating different SAR class types and this fact has been approved by several recent researches such as [16] and [17], which concluded that employing multiple features and different combinations can significantly improve the SAR image classification. Particularly a recent study [25] has shown that multi-feature combination using randomized clustering forest classifier can improve the classification performance up to 8%. Accordingly, we shall use a large set of features from both groups since feature scalability and optimal feature selection are the major objectives aimed by the proposed classification framework.

PolSAR systems often measure the complex scattering matrix, $[S]$, produced by a target under study with the

objective to infer its physical properties. Assuming linear horizontal and vertical polarizations for transmitting and receiving, $[S]$ can be expressed as,

$$[S] = \begin{bmatrix} S_{hh} & S_{hv} \\ S_{vh} & S_{vv} \end{bmatrix}. \quad (1)$$

Reciprocity theorem applies in a monostatic system configuration, $S_{hv} = S_{vh}$. For coherent scatterers only, the decompositions of the measured scattering matrix $[S]$ can be employed to characterize the scattering mechanisms of such targets. One way to analyze coherent targets is the Pauli decomposition, which expresses $[S]$ in the so-called Pauli basis. Hence by means of the Pauli decomposition, all polarimetric information in $[S]$ could be represented by combining the intensities $|\alpha|^2$, $|\beta|^2$ and $|\gamma|^2$, which determine the power scattered by different types of scatterers such as single- or odd-bounce scattering, double- or even-bounce scattering, and orthogonal polarization by volume scattering.

Alternatively, for nonstationary (distributed) targets, the second order polarimetric descriptors of the single-look polarimetric covariance $\langle [C] \rangle$ and coherency $\langle [T] \rangle$ matrices can be derived from $[S]$ and employed to extract physical information from the observed scattering process. Due to presence of speckle noise and random vector scattering from surface or volume, PolSAR data are often multi-look processed by averaging n neighboring pixels. By using the Pauli based scattering matrix for a pixel i , $k_i = [S_{hh} + S_{vv}, S_{hh} - S_{vv}, 2S_{hv}]^T / \sqrt{2}$, the multi-look coherency matrix $\langle [T] \rangle$ can be written as

$$\langle [T] \rangle = \frac{1}{n} \sum_{i=1}^n k_i k_i^{*T}. \quad (2)$$

Both coherency $\langle [T] \rangle$ and covariance $\langle [C] \rangle$ matrices are 3x3 Hermitian positive semidefinite matrices, and since they can be converted into one another by a linear transform, both are equivalent representations of the target polarimetric information.

The Cloude-Pottier decomposition is based on eigenanalysis of the polarimetric coherency matrix, $\langle [T] \rangle$:

$$\langle [T] \rangle = \lambda_1 e_1 e_1^{*T} + \lambda_2 e_2 e_2^{*T} + \lambda_3 e_3 e_3^{*T} \quad (3)$$

where $\lambda_1 > \lambda_2 > \lambda_3 \geq 0$ are real eigenvalues and the corresponding orthonormal eigenvectors e_i (representing three scattering mechanisms) are

$$e_i = e^{i\theta_i} \begin{bmatrix} \cos \alpha_i, \sin \alpha_i \cos \beta_i e^{i\delta_i}, \sin \alpha_i \sin \beta_i e^{i\gamma_i} \end{bmatrix}^T. \quad (4)$$

Cloude and Pottier defined entropy H , average of set of four angles $\bar{\alpha}$, $\bar{\beta}$, $\bar{\delta}$, and $\bar{\gamma}$, and anisotropy A for analysis of the physical information related to the scattering characteristics of a medium:

$$H = - \sum_{i=1}^3 p_i \log_3 p_i \quad \text{where} \quad (5)$$

$$p_i = \frac{\lambda_i}{\sum_{i=1}^3 \lambda_i},$$

$$\bar{\alpha} = \sum_{i=1}^3 p_i \alpha_i, \quad \bar{\beta} = \sum_{i=1}^3 p_i \beta_i, \quad (6)$$

$$\bar{\delta} = \sum_{i=1}^3 p_i \delta_i, \quad \bar{\gamma} = \sum_{i=1}^3 p_i \gamma_i$$

$$A = \frac{p_2 - p_3}{p_2 + p_3}. \quad (7)$$

Additionally, information about target's total backscattered power can be determined by the *Span* as,

$$Span = \sum_{i=1}^3 \lambda_i. \quad (8)$$

Entropy (H), estimate of the average alpha angle ($\bar{\alpha}$), and *Span* calculated by the above noncoherent target decomposition method have been commonly used as polarimetric features of a scatterer in many target classification schemes [14], [15].

Additionally, the complex correlation coefficients (ρ_{12} , ρ_{13} , ρ_{23}) between scattering matrix terms, which are important parameters in PolSAR data, can be included in the feature vector to be used as the input to the CNBC framework. As a result, we formed the following three set of feature vectors (FV_n), which will be input (sub-)features to the proposed network of binary classifiers detailed in Section 2. Each FV has the following components selected from the aforementioned features:

$$FV_1 = [T_{11}, T_{22}, T_{33}, C_{11}, |C_{12}|, \angle C_{12}, |C_{13}|, \angle C_{13}, C_{22}, |C_{23}|, \angle C_{23}, C_{33}] \quad (9)$$

$$FV_2 = [Span, H, A, \bar{\alpha}, \bar{\beta}, \bar{\delta}, \bar{\gamma}, \lambda_1, \lambda_2, \lambda_3] \quad (10)$$

$$FV_3 = [|\rho_{12}|, \angle \rho_{12}, |\rho_{13}|, \angle \rho_{13}, |\rho_{23}|, \angle \rho_{23}] \quad (11)$$

For the purpose of normalizing and scaling each feature vector, first the logarithm of magnitude features in FV₁, and *Span* and three eigenvalues in FV₂ are taken before all features are linearly scaled into [-1, 1] interval. Note that while calculating the logarithm, features with zero values are replaced with their respective nonzero

minimum. Finally, histogram equalized feature vectors that are found to be more effective using the FV visualization application as explained next, can then be presented to the input layer of the proposed CNBC.

4. EXPERIMENTAL RESULTS

Two benchmark PolSAR images were used for qualitative and numerical performance evaluations. The first one is the NASA/Jet Propulsion Laboratory Airborne SAR (AIRSAR) L-band data of the San Francisco Bay (SFBay). The original four-look fully polarimetric SAR data of the San Francisco Bay, having a dimension of 900x1024 pixels, provides good coverage of both natural (sea, mountains, forests, etc.) and man-made targets (buildings, streets, parks, golf course, etc.) We defined 5 distinct classes for both natural (such as *water - sea*, *mountain - cliffs*, *forest - trees*, *flat zones* such as beach, grass etc.) and *urban* area (buildings, streets, roads, etc.) targets with a more complex inner structure. Furthermore, for numerical evaluation the L-band PolSAR dataset of Flevoland, The Netherlands is used to perform crop and land classification. This dataset has a size of 1024x750 pixels and collected in mid-August 1989 during MAESTRO-1 Campaign. There are 12 ground-truth classes in this dataset: *water*, *forest*, *stem beans*, *lucerne*, *roads*, *bare soil*, *grass*, *peas*, *rapeseed*, *beet*, *potatoes* and *wheat* [1]. Over both datasets, the speckle filter suggested by Lee *et al.* [13] is employed within a 5x5 window.

The CNBCs created and evolved for each SAR image contains number of NBCs, which is equivalent to the number of those pre-defined classes (i.e. 5 for the SF Bay and 10/12 for the Flevoland data). Recall that each NBC in both CNBCs, contains certain number BCs in the input layer, which is equivalent to the number of FV sets. Therefore, each NBC has 4 BCs (3 in the input layer + the fuser BC) and thus a total of $4 \times 5 = 20$ classifiers for SF Bay and $4 \times 10 = 40$ ($4 \times 12 = 48$) classifiers for Flevoland data are individually evolved using Multi-Layer Perceptrons over exhaustive Back Propagation (BP) in this paper. Furthermore, note that for each BC, its input size is determined by the size of its FV, i.e. 12, 10 and 6 for the input layer BCs of all NBCs and naturally, $3 \times 2 = 6$ for all fuser BCs.

The evolution (and training) parameters and internal settings of the MLPs are as follows: the learning parameter for BP is $\eta = 0.002$, the iteration number is 1000, and the activation function is the hyperbolic tangent. For the MLP AS, we used the simplest configurations within the following range arrays: $R_{\min} \{N_i, 8, 2\}$ and $R_{\max} \{N_i, 16, 2\}$, which indicate that besides the single layer perceptron, all MLPs have only a single hidden layer with 8 to 16 hidden neurons. Note that the input N_i depends on the size of FV_n . Finally, for the evolution method which seeks for the optimal configuration in the AS, 10 independent BP runs for each configuration in the AS are performed and the best one is selected.

For the first benchmark SAR image, SF Bay, the ground-truth data (GTD) and the classification results are shown in Figure 3. The GTD, which is equal to the training dataset used contains only 1305 pixels, which correspond to just $\sim 0.15\%$ of the entire SAR data and its accuracy cannot be not 100% guaranteed. We can at best assume that the *majority* of those points belong to the classes they are assigned to.

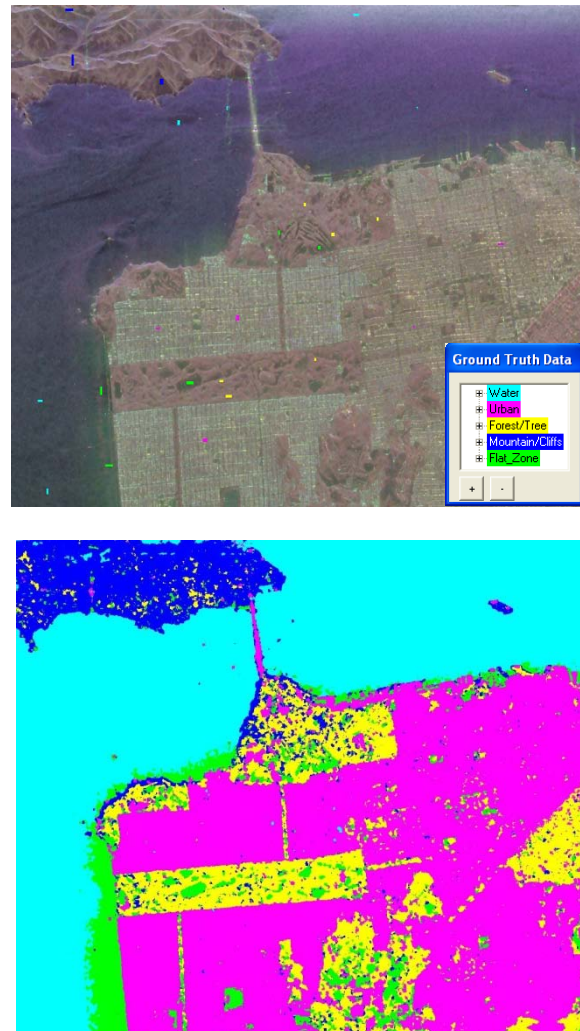


Figure 3: SFBay GTD and the proposed CNBC classifications 5 classes - {water:cyan, urban:pink, forest:yellow, flat zone: green, mountain: blue }.

For comparative evaluations classification results from some of major techniques a 3-layer ANN [24] and Optimization of Polarimetric Contrast Enhancement (OPCE) [22], are shown in Figure 4 (bottom-row) with their class equivalents of the proposed CNBC with 758 and 1058 GTD data, respectively (top-row).

The 3-layer ANN is applied only over a sub-area (600x600 pixels) of the SAR image with 3 classes, *water*, *urban* and *forest*, see Figure 4, bottom-left. They used more than 26000 pixels for training with a 19-D feature vector which has been reduced to 10-D by PCA. Although with minimal number of classes used and a massive size of training samples, it is evident that this

method has large misclassified sections, particularly in the *water* and *mountain* (or *forest*) terrains. OPCE is also applied over a sub-area of 700x900 pixels (Figure 4, bottom-right) with 4 classes, *water*, *urban*, *forest* (or woods) and quasi-natural (equivalent of *flat zone* class in the current work), and still suffered from excessive noise and misclassified sections in the *sea* and *mountain* (or *forest*) terrains.

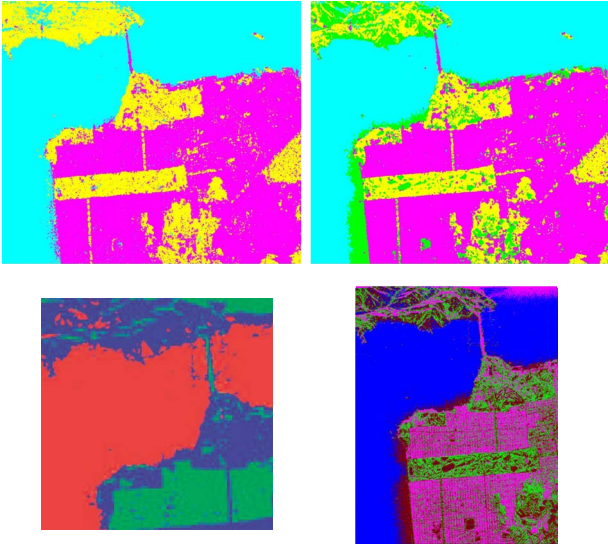


Figure 4: Classification results of CNBC 3 and 4 classes (top-row)- {water:cyan, urban:pink, forest:yellow, flat zone: green}, ANN-based (bottom-left) - { water:red, urban:green, forest:blue} and OPCE (bottom-right) - {water:cyan, urban:pink, forest:yellow, flat zone:green, mountain:blue}.

The Flevoland dataset allows us to perform numerical evaluations of the classification performance of the proposed CNBC since it has a publicly available ground truth data (GTD) with the aforementioned 12 classes. This GTD, as shown in Figure 5, contains 173611 pixels, 8658 of which were selected as the training dataset. Our classification maps are shown in Figure 6.

For comparative evaluations, we compare the overall classification accuracy with the results of the classification methods over the same (Flevoland) data reported recently in [5]. Although it has the same GTD, there are four major differences. First, those methods used only a limited part of the GTD available, i.e. 47037 pixels for training and (only) 41278 pixels for testing, so a mere total of 88315 whereas our GTD size is roughly double of this figure. Second, in their work only 10 classes are used, excluding roads and merging Peas and Beet into a single class whereas we treat them separately as in [1]. We also used their 10 class scheme for comparison. Thirdly, all classifiers are trained with a massive size of the overall GTD data (47037) whereas we used around 1/6 of this (7515) to classify the test region, which is roughly four times (171974) larger than they used. Finally, their selected training and test sets are really close to each other, which may bias test set

accuracy. Table 1 presents the overall accuracies achieved by Normal Distribution Maximum Likelihood (NML) from [5], Extraction and Classification of Homogenous Objects (ECHO) from [5] and the proposed CNBC over 3 different feature sets namely 6I+3P (6 intensity and 3 phase images from T), H/A/ $\bar{\alpha}$ (H/A/ $\bar{\alpha}$ features from the Cloude-Pottier Decomposition) and 6I+H/A/ $\bar{\alpha}$ (6 intensity images from T and H/A/ $\bar{\alpha}$). For further comparison, we also show the results using our test set for the 10 (C10) and 12 (C12) class cases.



Figure 5: Flevoland ground truth data for 12 classes



Figure 6: Classification map for proposed CNBC with MLP-BP over 10 (top) and 12 classes (bottom).

Table 1 - Overall accuracies for the 3 classification methods over test datasets

	6I+3P	H/A/$\bar{\alpha}$	6I+H/A/$\bar{\alpha}$	28D FV
NML	0.666	0.325	-	-
ECHO	0.813	0.526	0.770	-
CNBC C10	0.697	0.718	0.850	0.926
CNBC C12	0.666	0.729	0.834	0.892

Although it is probably unfair to make direct performance comparison between the proposed CNBC classifier and these compared methods due to the unbalanced train - test dataset sizes and the different number of classes they used, the proposed technique still achieved better accuracy on two out of three feature sets for C10 and a superior classification accuracy using an extended feature set. Even the best competing classifier, the ECHO-(6I+3P), is short of ~11% and ~8% for C10 and C12 from the CNBC’s classification accuracy level and it is an expected outcome that the performance gap

would be further increased if the comparative evaluations were performed under equal terms. This is basically the advantage of using as many features as possible since the proposed CNBC can use the individual discrimination power of each of them whilst compensating their weaknesses with the others, and thus it can further improve the overall classification performance with incremental contribution of each individual feature.

As presented in the confusion matrix in

Table 2, the proposed CNBC can distinguish each individual class reasonably well in the test dataset except perhaps few classes such as *potato – forest* (and vice versa), *roads – grass* and especially *wheat – rapeseed* (and vice versa). The reason for this is the lack of discrimination between those classes presented by the current features used and hence the need for new feature(s), which can better discriminate these classes, is imminent so as to significantly improve the overall classification performance.

Table 2 - Confusion matrix for test set over CNBC C12. Highest classification errors are marked.

	Water	Forest	Stem Beans	Lucerne	Grass	Bare_Soil	Rapeseed	Beet	Potato	Wheat	Peas	Roads	Size	CA
Water	27994	2	5	187	29	253	44	3	15	17	6	694	29249	0,9571
Forest	0	9203	48	19	0	0	0	103	1256	45	0	323	10997	0,8369
Stem_Beans	0	67	6934	72	0	0	1	120	135	163	6	437	7935	0,8739
Lucerne	0	14	0	9396	217	0	2	31	34	24	0	1112	10830	0,8676
Grass	0	25	21	317	7958	0	18	87	6	74	6	1223	9735	0,8175
Bare_Soil	67	1	5	3	34	5755	23	6	0	2	0	188	6084	0,9459
Rapeseed	7	13	9	2	12	2	19460	42	0	1759	210	845	22361	0,8703
Beet	0	261	90	56	7	0	156	9883	256	185	110	662	11666	0,8472
Potato	0	1366	266	40	4	0	4	925	16575	150	34	637	20001	0,8287
Wheat	1	20	7	58	82	1	972	82	0	30567	136	798	32724	0,9341
Peas	1	7	5	0	0	0	353	122	3	333	9416	152	10392	0,9061
Roads	0	27	8	69	197	0	41	11	1	35	10	1238	1637	0,7563

5. CONCLUSIONS

In this paper, a novel CNBC scheme is introduced to address the PolSAR image classification problem with the primary objective of maximizing accuracy and efficiency. The proposed scheme mainly adopts a “Divide and Conquer” type of approach, so as to handle efficiently indefinite number of SAR features and classes, which otherwise turn out to be difficult, if not infeasible problem for a single classifier due to the well known “curse of dimensionality” phenomenon. In the proposed framework approach, compact classifiers, which can be evolved and trained in a much more efficient way than a single but complex classifier, can be conveniently used in the architecture space, in which the optimum classifier for the classification problem in hand can be searched with the proposed evolutionary techniques. At a given time, this allows to create a dedicated classifier (BC) for discriminating a certain class type from the others with the use of a single (sub-) feature. Each (incremental) evolution session “learns” from the current best classifier and can improve it further, possibly with another configuration in the

architecture space. Moreover, with each incremental evolution, new classes/features can also be introduced which signals CNBC to create new corresponding NBCs and BCs to adapt dynamically to the change. In this way the CNBC can dynamically adapt itself to a classification problem whilst striving for maximizing the classification accuracy.

The experimental results, first of all, show a better performance of the CNBC framework in terms of classification accuracy, despite the ground-truth data may not be 100% accurate and the training dataset may contain only a mere fraction (0.2% or even less) of the available polarimetric SAR data. The former basically shows the robustness against training dataset errors and the latter indicates a high level of learning and generalization ability with the least amount of data. The comparative evaluations with several single-classifier methods presents that a significant performance gap occurs despite of the fact that they have the advantage of classifying less number of classes, whilst having a much smaller test, yet an significantly larger training datasets. Although the results indicate that all the aforementioned objectives have been successfully fulfilled, even higher

accuracy levels can still be expected from the CNBC framework with the addition of new powerful SAR features such as the Yamaguchi and the van Zyl decompositions and spatial descriptors extracted by image processing techniques (i.e. color, texture, edge). With such high accuracy levels, we can further foretell that a CNBC evolved for one SAR image can then be used “as is” or perhaps with minimal incremental evolutions, to classify another SAR images with similar terrain classes. Also we will investigate other polarimetric SAR image types from different airborne and space-borne systems and this can even be further extended into a retrieval framework for SAR image databases where SAR image(s) with certain class type(s) can be queried and retrieved. These are all subject to our future work.

ACKNOWLEDGEMENT

This work was supported by the Academy of Finland, project No. 213462 (Finnish Centre of Excellence Program, 2006-2011). The authors would also like to thank the ESA/ESRIN for making the used dataset available as part of the Polarimetric SAR Data Processing and Educational Tool (POLSTARPRO).

REFERENCES

- [1] Ainsworth, T.L., Kelly, J.P. & Lee J.-S. (2009). Classification comparisons between dual-pol, compact polarimetric and quad-pol SAR imagery. *ISPRS Journal of Photogrammetry and Remote Sensing*. **64**(5), 464-471.
- [2] Bruzzone, L., Marconcini, M., Wegmuller, U. & Wiesmann, A. (2004). An advanced system for the automatic classification of multitemporal SAR images. *IEEE Transactions on Geoscience and Remote Sensing*. **42**(6), 1321-1334.
- [3] Cameron, W. L., Youssef, N. N. & Leung, L. K. (1990). Feature motivated polarization scattering matrix decomposition. *Proceedings of IEEE International Radar Conference*, Arlington, VA, USA, pp549-557.
- [4] Cloude, S. R. & Pottier, E. (1996). A review of target decomposition theorems in radar polarimetry. *IEEE Transactions on Geoscience and Remote Sensing*. **34**(2), 498-518.
- [5] Chen, E., Li, Z., Pang, Y. & Tian, X. (2007). Quantitative Evaluation of Polarimetric Classification for Agricultural Crop Mapping. *Photogrammetric Engineering and Remote Sensing*, **73**(3), 279-284.
- [6] del Frate, F., Pacifici, F., Schiavon, G., & Solimini, C. (2007). Use of Neural Networks for Automatic Classification From High-Resolution Images. *IEEE Transactions on Geoscience and Remote Sensing*, **45**(4), 800-809.
- [7] Freeman, A. & Durden, S. L. (1998). “A three-component scattering model for polarimetric SAR data. *IEEE Transactions on Geoscience and Remote Sensing*. **36**(3), 963-973.
- [8] Huynen, J. R. (1970). Phenomenological Theory of Radar Targets. Ph.D. Dissertation, Tech. Univ. Delft, Delft, The Netherlands.
- [9] Kiranyaz, S., Ince, T., Yildirim, A. & Gabbouj, M. (2010). Fractional Particle Swarm Optimization in Multi-Dimensional Search Space. *IEEE Transactions on Systems, Man, and Cybernetics – Part B*. **40**(2), 298-319.
- [10] Kiranyaz, S., Ince, T., Yildirim, A. & Gabbouj, M. (2009). Evolutionary Artificial Neural Networks by Multi-Dimensional Particle Swarm Optimization. *Neural Networks*, **22**(10), 1448-1462.
- [11] Krogager, E. (1990). A new decomposition of the radar target scattering matrix. *Electronics Letters*. **26**(18), 1525-1526.
- [12] Krogager, E. & Czyz, Z. H. (1995). Properties of the sphere, diplane, helix (target scattering matrix decomposition). *Proceedings of 3rd International Workshop on Radar Polarimetry*. Nantes, France, pp106-114.
- [13] Lee, J. S., Grunes, M. R. & Kwok, R. (1994). Classification of multi-look polarimetric SAR imagery based on complex Wishart distribution. *International Journal of Remote Sensing*. **15**(11), 2299-2311.
- [14] Lee, J. S., Grunes, M. R., Ainsworth, T., Du, L.-J., Schuler, D. & Cloude S. R. (1999). Unsupervised classification using polarimetric decomposition and the complex Wishart classifier. *IEEE Transactions on Geoscience and Remote Sensing*. **37**(5), 2249-2257.
- [15] Liu, G., Xiong, H. & Huang, S. (2007). “Study on segmentation and interpretation of multi-look polarimetric SAR images. *International Journal of Remote Sensing*. **21**(8), 1675-1691.
- [16] She, X. L., Yang, J. & Zhang, W. J. (2007). The boosting algorithm with application to polarimetric SAR image classification. *Proceedings of the 1st Asian and Pacific Conference on Synthetic Aperture Radar*. Huangshan, China, pp779-783.
- [17] Shimoni, M., Borghys, D., Heremans, R., Perneel, C., & Acheroy, M. (2009). Fusion of PolSAR and PolInSAR data for land cover classification. *International Journal of Applied Earth Observation and Geoinformation*. **11**(3), 169-180.
- [18] Pottier, E. & Lee, J.S. (2000). Unsupervised classification scheme of POLSAR images based on the complex Wishart distribution and the H/A/alpha-Polarimetric decomposition theorem. *Proceedings of the 3rd European Conference on Synthetic Aperture Radar*. Frankfurt, Germany, pp265-268.
- [19] Tan, C. P., Lim, K. S. & Ewe, H. T. (2007). Image processing in polarimetric SAR images using a hybrid entropy decomposition and maximum likelihood (EDML). *Proceedings of International Symposium on Image and Signal Processing and Analysis*. Istanbul, Turkey. pp418-422.
- [20] Wu, Y., Ji, K., Yu, W. & Su, Y. (2008). Region-based classification of polarimetric SAR images using Wishart MRF. *IEEE Geoscience and Remote Sensing Letters*. **5**(4), 668-672.
- [21] Ye, Z. & Lu, C.-C. (2002). Wavelet-Based Unsupervised SAR Image Segmentation Using Hidden Markov Tree Models. In *Proceedings of the 16th International Conference on Pattern Recognition*. Quebec, Canada, pp729-732.
- [22] Yin, J. J., Yang, J. & Yamaguchi, Y. (2009). A new method for polarimetric SAR image classification. *Proceedings of the 1st Asian and Pacific Conference on Synthetic Aperture Radar*. Xian, China, pp733-737.
- [23] Yang, S. Y., Wang, M. & Jiao, L. C. (2009). Radar target recognition using contourlet packet transform and neural network approach. *Signal Processing*, **89**(4), 394-409.
- [24] Zhang, Y. D., Wu, L.-N. & Wei, G. (2009). A new classifier for polarimetric SAR images. *Progress In Electromagnetics Research*. **94**, 83-104.
- [25] Zou, T., Yang, W., Dai, D. & Sun H. (2009). Polarimetric SAR Image Classification Using Multifeatures Combination and Extremely Randomized Clustering Forests. *EURASIP Journal on Advances in Signal Processing*, vol. 2010, Article ID 465612.
- [26] van Zyl, J. J. (1989). Unsupervised classification of scattering mechanisms using radar polarimetry data. *IEEE Transactions of Geoscience and Remote Sensing*. **27**(1), 36-45.